Dental Materials 41 (2025) 383–390

Contents lists available at ScienceDirect

Dental Materials

journal homepage: www.elsevier.com/locate/dental

Effect of mechanical instrumentation on titanium implant surface properties

Mohammed Alabbad [a,b,*], Nick Silikas [a], Andrew Thomas [c,d]

[a] Division of Dentistry, School of Medical Sciences, University of Manchester, Manchester M13 9PL, UK
[b] Department of Periodontics, Faculty of Dentistry, King Abdulaziz University, Jeddah 21589, Saudi Arabia
[c] Department of Materials, School of Natural Sciences, University of Manchester, Manchester M13 9PL, UK
[d] Photon Science Institute, University of Manchester, Manchester M13 9PL, UK

ARTICLE INFO

Keywords:
Peri-implantitis
Peri-implantitis treatment
Decontamination
Mechanical treatment
Physical decontamination
Titanium brush
Surface roughness
Wettability
EDX
SLA

ABSTRACT

Objective: To assess the impact of mechanical decontamination using rotary brushes on the surface topography, elemental composition, roughness, and wettability of titanium implant surfaces.

Methods: Four commercially available rotary brushes were used: Labrida BioClean Brush® (LB), i-Brush1 (IB), NiTiBrush Nano (NiTiB), and Peri-implantitis Brush (PIB). Seventy-five titanium discs with sandblasted, large-grit, acid-etched (SLA) surfaces were randomly assigned to five groups ($n = 15$): LB, IB, NiTiB, PIB, and a control group. Each disc was treated for 60 seconds with the respective rotary brush according to the manufacturer's instructions. Surface morphology was analysed using Scanning Electron Microscopy (SEM), surface elemental composition with Energy Dispersive X-ray (EDX), surface roughness via optical profilometry, and wettability with a droplet shape analyser.

Results: SEI analysis revealed morphological changes, including scratches, flattening, and loose titanium particles in the IB, PIB, and NiTiB groups, whereas the LB group preserved the original surface morphology. SEM-EDX analysis showed that LB, PIB, and NiTiB groups closely match the control elemental composition. However, IB groups showed significantly different composition. Surface roughness values in the IB, PIB, and NiTiB groups differed significantly from the control ($p < 0.05$), whereas the LB group had comparable roughness values ($p > 0.05$). Contact angle measurements indicated enhanced wettability in IB, PIB, and NiTiB groups ($p < 0.05$), while the LB group exhibited values comparable to the control ($p > 0.05$).

Significance: Mechanical decontamination of implant surfaces utilising rotary brushes can alter implant surface properties.

1. Introduction

Dental implant placement has become a routine clinical procedure for replacing missing teeth, with high predictability and long-term survival rates [1,2]. However, the prolonged functional lifespan of dental implants inevitably increases the probability of developing prosthetic and biological complications in patients [3–6]. Peri-implantitis is one of the most frequent biological complications affecting the soft and hard tissue surrounding the dental implant [4–7]. It is widely recognised that bacterial colonisation on the implant surface as an adherent biofilm is the primary etiological factor for peri-implantitis [8–10]. The treatment modalities for managing peri-implantitis are broadly categorised into non-surgical and surgical therapies [11,12]. Both modalities involve implementing surface decontamination techniques to eliminate the adherent biofilm and calculus on the implant surface. Numerous approaches have been proposed to decontaminate the implant surface, including mechanical, chemical, laser, electrolysis, and implantoplasty [13]techniques. Mechanical debridement is advocated in numerous clinical protocols and recommended in the clinical practice guidelines for the prevention and treatment of peri-implant diseases [11–15]. The mechanical tools used to decontaminate the implant surface should eliminate soft and hard deposits without producing detrimental changes on the implant surface [16,17]. It is well known that surface properties such as surface roughness, surface free energy, and chemical

* Correspondence to: University of Manchester, School of Medical Sciences, Division of Dentistry, Coupland 3 Building, Oxford Road, Manchester M13 9PL, UK.
E-mail addresses: mohammed.alabbad@postgrad.manchester.ac.uk (M. Alabbad), nikolaos.silikas@manchester.ac.uk (N. Silikas), andrew.g.thomas@manchester.ac.uk (A. Thomas).

https://doi.org/10.1016/j.dental.2024.12.014
Received 27 October 2024; Received in revised form 10 December 2024; Accepted 22 December 2024
Available online 9 January 2025

composition influence cellular responses and bacterial colonisation [18–22]. Osteogenic cells and bacteria favour attachment to moderately rough surfaces [23–25]. On the other hand, epithelial and gingival cells have a better affinity toward smooth surfaces [26,27]. Implant surfaces are also modified to improve their chemical composition, surface charge, and surface energy, which are crucial for cell attachment and protein adsorption [28,29]. Therefore, any surface alteration following mechanical debridement may affect the subsequent desired cellular responses and bacterial adhesion. Different tools are used to decontaminate the implant surface mechanically, such as plastic and metal curettes, ultrasonic scalers, and air-abrasive systems. The effects of utilising these tools to decontaminate implant surfaces have been evaluated in the literature [16,30,31]. Plastic curettes and ultra-sonic scalers with plastic tips were found ineffective in debriding the implant surface, and plastic remnants were detected on the surface[16,31]. On the other hand, metal curettes and ultrasonic scalers with metal tips have been shown to be effective in debriding the implant surface. However, their use results in significant surface alteration[16,31]. Air-abrasive systems are effective in debriding implant surfaces with minimal alterations; however, concerns regarding restoring surface biocompatibility exist in the literature [30,32–35]. The treatment of peri-implantitis has limited predictability due to incomplete surface decontamination attributed to the complex implant surface topography, including macro and micro features [36,37]. Recently, dental professionals are increasingly using rotary brushes for decontaminating implant surfaces [38–41]. It is believed that rotary brushes are composed of gentle bristles that better adapt to the implant surface and can decontaminate implant surfaces efficiently with minimal or no surface alterations [42]. According to clinical evaluations, rotary brushes are safe for treating peri-implantitis; however, their influence on implant surface characteristics remains inadequately explored [43–47]. Additionally, the existing literature compares the effect of rotary brushes to other mechanical tools yet lacks a direct comparison between different rotary brushes. The aim of this study is to compare the surface alteration caused by four commercially available rotary brushes used to decontaminate titanium implant surfaces. The specific objectives were to assess: i) surface damage qualitatively (visual and SEM); ii) surface elemental composition changes (SEM-EDX analysis); iii) changes in surface roughness; and iv) wettability. The null hypothesis is that the use of rotary brushes for implant surface decontamination does not alter implant surface properties.

2. Materials and methods

2.1. Titanium substrate preparation

Machined titanium discs (Grade 5 Ti 6Al-4V; Zimmer Biomet, Barcelona, Spain) of 14.5 mm diameter and 2 mm thickness were used as titanium substrates. Discs were sandblasted for 30 s using aluminium oxide particles of 150 microns in size. Following sandblasting, discs were acid etched in a boiling mixed solution of hydrochloric acid (37 wt %), sulfuric acid (98 wt%), and ultrapure water for 5 minutes. Discs were cleaned sequentially in an ultrasonic bath using ultrapure water, pure acetone, and pure ethanol; then rinsed with ultrapure water and dried at room temperature. The prepared discs were moderately rough (Sa (average roughness) 1.5 μm) with a Sandblasted, Large-Grit, and Acid-Etched (SLA) surface Fig. 1.

2.2. Decontamination groups

Four commercially available rotary brushes were used in this study, as shown in Table 1 and Fig. 2. All prepared SLA discs (n = 75) were randomly divided into four decontamination groups and a control (n = 15). Each disc was instrumented for 60 s under copious irrigation following the manufacturers' guidelines. The average force in this experiment was similar to that applied in a clinical setting.

2.3. Surface characterisation

2.3.1. Surface morphology

The gross surface alterations were observed by the naked eye and photographed (EOS 600D, CANON, Japan). The topographic surface evaluation was performed using a Field Emission Scanning Electron Microscope (FE-SEM)(Quanta FEG 250, FEI Company, Hillsboro, Oregon, USA). The discs did not require any coating and were mounted on SEM stubs with conductive carbon adhesive discs (Agar Scientific Ltd, Essex, England, UK). The evaluation was conducted at variable magnifications operating in high vacuum mode, at an accelerating voltage of 20 kV, an emission current of 148 μA, and a working distance of 10 mm. Images were obtained using a secondary electron detector (SED). Microscopy was performed on five discs of each group.

Table 1
Experimental rotary brushes and manufacturers' information.

Name	Abbreviation	Manufacturer	Bristles material	Instrumentation
Labrida BioClean®	LB	Labrida AS, Oslo, Norway	Marine polymer	Brush was soaked in a saline for 2 mins. Discs instrumented at 1000 rpm[1] in a probing motion.
i-Brush1	IB	Neo Biotech, Seoul, Republic of Korea.	Stainless steel	Discs instrumented at 5500 rpm[2] in a unidirectional movement.
NiTiBrush Nano	NiTiB	HANS, Gyeonggi, Republic of Korea.	Nickel-titanium	Discs instrumented at 800 rpm[3] in a unidirectional movement.
Peri-implantitis brush	PIB	SOWDANE, Mainland, China.	Titanium	Discs instrumented at 2000 rpm in a unidirectional movement.

[1] A midrange was chosen for the recommended rotational speed (< 2000).
[2] A midrange was chosen for the recommended rotational speed (2000–9000).
[3] A midrange was chosen for the recommended rotational speed (600–1000).

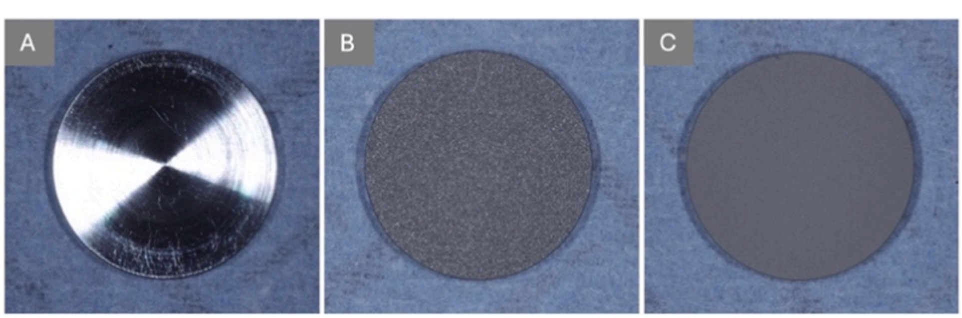

Fig. 1. Gross view of titanium discs. (A) Machined titanium disc. (B) Titanium disc after sandblasting. (C) Titanium disc with SLA surface.

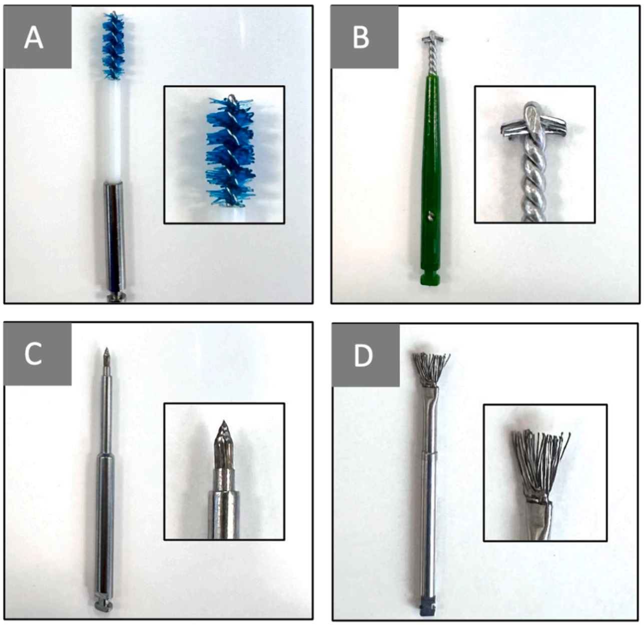

Fig. 2. Rotary brushes used in this study. (A) Labrida BioClean® (LB), (B) i-Brush1 (IB), (C) NiTiBrush Nano (NiTiB), (D) Peri-implantitis Brush (PIB).

2.3.2. Surface elemental composition

The surface elemental composition was determined using Energy-Dispersive X-ray Spectrometry (SEM-EDX; X-Max, Oxford Instruments, Oxford, England). The measurements were performed at 20 kV, with a working distance of 10 mm, at 1kx magnification. Images were captured and mapped using specialised software (Aztec 3.3, Oxford Instruments, Oxford, England). Five discs of each group were evaluated at five random areas on each disc (n = 125, 25 measurements per group) to identify the elemental composition and calculate their atomic weight (wt%).

2.3.3. Surface roughness

A 3-D optical surface profilometer (TopMap Micro.View, Polytech, Baden-Württemberg, Germany) was used to assess the surface roughness. Before measurement, the discs underwent ultrasonic cleaning in ultrapure water to remove any loose particles on the surface resulting from the mechanical brushing. The evaluation was carried out on five discs of each group, and measurements were obtained from five random areas of each disc (n = 125, 25 measurements per group). Each surface scan covered an area of 392.63 × 290.43 µm, and surface values were determined using a Gaussian filter with a cut-off length of 0.04 µm. Surface roughness parameters were then calculated using specialised software (TMS 4.2, Polytech, Baden-Württemberg, Germany). The surface was analysed using three-dimensional parameters, as suggested by Wennerberg and Albrektsson [48], following ISO standards (ISO 25178–2:2012):

(Sa): arithmetical mean height; (Sz): maximum height; (Ssk): skewness; (Sku): kurtosis; (Sdq): root mean square gradient; and (Sdr): developed interfacial area ratio.

2.3.4. Surface wettability

To evaluate the surface wettability, a droplet shape analyser (Dropometer, Droplet Lab, Canada) was employed to determine the contact angles. An automated dispenser, preloaded with ultrapure water, was utilised to deposit a droplet of 3 µl onto each treated surface at an ambient temperature of 23 °C. After 5 s of depositing the water droplet, digital images were captured. The images were analysed using dedicated software that utilises a polynomial fit to calculate the contact angle on the right and left sides. Contact angle measurements were taken from five discs in each group, with five repeat measurements obtained for each disc (n = 125, 25 measurements per group). The mean contact angle was then computed for each group to yield a representative value for analysis.

2.4. Statistical analysis

The required sample size was calculated using G*Power software (V. 3.1.3; Heinrich Hein University, Germany) based on a pilot study to achieve a 90 % power probability with significance set at 0.05. Therefore, five samples/ per group for surface roughness, wettability, and elemental composition were chosen. The obtained data were analysed using statistical software (SPSS 29.0; IBM SPSS Statistics Inc., Chicago, IL, USA). Data were tested for normality and homogeneity of variance using the Shapiro-Wilk and Levene's tests, respectively. Normality assumptions were violated, hence the differences among the decontamination groups were investigated using the Kruskal-Wallis followed by Dunn-Bonferroni pairwise multiple comparison tests ($p < 0.05$). To investigate the association between surface roughness parameters, Spearman's rank correlation coefficient (r_s) was computed.

3. Results

3.1. Surface morphology

3.1.1. Visual inspection

The gross view of titanium discs following treatment with the brushes is depicted in Fig. 3. Upon examination, the LB group exhibits faint marks of mechanical brushing; however, the changes are not distinguishable from the control group. On the other hand, the IB, NiTiB,

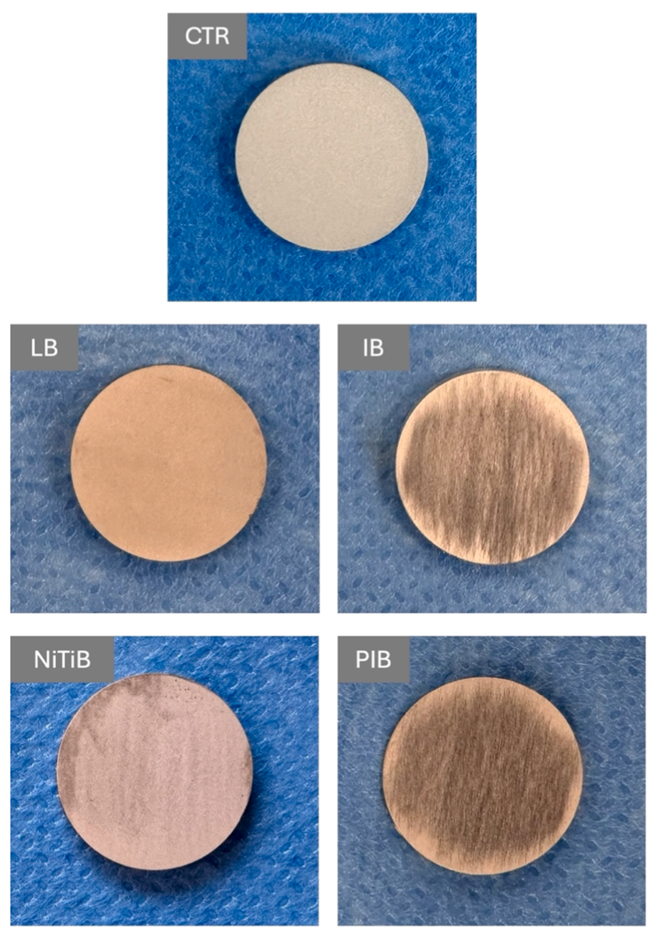

Fig. 3. Gross view of titanium discs following mechanical instrumentation.

and PIB groups show significant macroscopic surface alterations in the form of surface scratches. The degree of surface scratching varies among the groups, where IB and PIB groups show noticeable surface scratches, while these are less evident in the NiTiB group.

3.1.2. SEM

The secondary electron images (SEI) of all decontamination groups are presented in Fig. 4. The control group displays the characteristic honeycomb-like structure of the SLA surface. The LB group resembles the control with minimal changes. Conversely, IB, NiTiB, and PIB groups exhibit significant surface alterations. Flattened, island-like features replace portions of the honeycomb structure. These islands appeared scattered randomly in IB, NiTiB, or directionally aligned in PIB. Higher magnification reveals scratches on the flattened areas, consistent with brush rotation. Debris, likely abraded titanium particles, is observed on IB, NiTiB, and PIB surfaces. All groups display a mix of flattened areas and remaining honeycomb structures, with decreasing visibility of the original features in this order: CTR = LB > NiTiB > IB > PIB.

3.2. Surface elemental composition

SEM-EDX identifies the presence of titanium (Ti), aluminium (Al), vanadium (V), and oxygen (O) as the key elemental components of the control SLA surface. Fig. 5 shows the average atomic weights (wt%) for these elements across all decontamination groups. LB, PIB, and NiTiB groups closely match the control composition, with minor fluctuations in element percentages. LB has a slight rise in carbon (C) content, while PIB and NiTiB show minor increases in titanium (Ti) concentration. Nickel (Ni) is present in trace amounts in the NiTiB group. In contrast, the IB group notably differs in elemental composition. SEM-EDX of the surfaces instrumented with IB reveal the presence of cobalt (Co), chromium (Cr), and molybdenum (Mo) as predominant elements on the surface, alongside iron (Fe), carbon (C), aluminium (Al), and traces of silicon (Si).

3.3. Surface roughness

Results for surface roughness parameters (Sa, Sz, Ssk, Sku, Sdq, and Sdr) are summarised in Table 2. The Kruskal-Wallis test indicates significant differences among the decontamination groups across all roughness parameters ($p < 0.001$). The Dunn-Bonferroni *post hoc* test was then applied. For **Sa**, the LB group shows similar measurements to the control ($p > 0.05$), while the IB, NiTiB, and PIB groups have significantly lower values ($p < 0.05$). The IB group has the most pronounced reduction (CTR = 1.51 ± 0.02, IB = 0.92 ± 0.16), with the following trend: CTR = LB > NiTiB > PIB > IB. Regarding **Sz**, the LB group is similar to the control ($p > 0.05$), whereas the IB, NiTiB, and PIB groups exhibit significantly lower values ($p < 0.05$), with comparable reductions among these three groups. For **Ssk**, the LB group matches the control ($p > 0.05$), but the IB, NiTiB, and PIB groups have significantly lower values ($p < 0.05$). The IB group has the greatest reduction (CTR = -0.25 ± 0.07, IB = -1.08 ± 0.41), with the trend: CTR = LB > PIB > NiTiB > IB. In terms of **Sku**, the LB and NiTiB groups are similar to the control ($p > 0.05$), while the IB and PIB groups have significantly higher values ($p < 0.05$). For **Sdq**, the NiTiB group match the control ($p > 0.05$), whereas the LB group has higher values, and the IB and PIB groups have significantly lower values ($p < 0.05$). The Sdq values follow the trend: LB > CTR = NiTiB > PIB > IB. Regarding **Sdr**, the LB group has higher values than the control ($p < 0.05$), while the IB, NiTiB, and PIB groups have significantly lower values ($p < 0.05$). The IB group has the greatest reduction in Sdr (CTR = 120.82 ± 4.23, IB = 68.79 ± 16.53), with the trend: LB > CTR > NiTiB > PIB > IB. There was a strong positive correlation between Sa and Sdr ($r_s = 0.891$, $p < 0.001$).

3.4. Surface wettability

Results for the contact angle measurements (θ) are presented in Table 2 and Fig. 6. The Kruskal-Wallis test indicated significant differences between the decontamination groups ($p < 0.001$). Further analysis showed that the LB group's contact angle was similar to the control ($p > 0.05$). In contrast, the IB, NiTiB, and PIB groups exhibited significantly higher wettability ($p < 0.05$) compared to the control, indicated by their significantly lower contact angles. The IB and PIB groups reduced the contact angle to a similar extent, while the NiTiB group reduced it to a lesser degree.

4. Discussion

In our study, four rotary brushes used for mechanical decontamination were tested on titanium samples with SLA surface to assess the effects on surface morphology, topography, elemental composition, and wettability. The null hypothesis was rejected.

4.1. Surface morphology

Our study shows that mechanical instrumentation using rotary brushes can induce significant surface alterations, such as scratches, flattening and deformation of the honeycomb structure. The scratches and grooves created by brushes could lead to plaque attachment and make calculus formation easier. These observations of surface deformation are not unique findings, and similar observations have been reported in the literature [49–52]. The extent of deformation seems to be related to the brush bristles material and design. In our study, PIB results in the most extensive surface damage, which is attributed to the tuft-like brush design incorporating many metallic bristles. The IB and NiTiB produced moderate surface damage due to fewer bristles in IB and the pointed tip design in NiTiB. In contrast, minimal surface alterations were observed with LB as its bristles were made of a soft marine polymer.

During SEI evaluation, titanium particles were observed over the titanium surfaces instrumented with IB, NiTiB, and PIB. These are likely to be wear particles generated as a direct effect of the mechanical instrumentation. In line with our findings, Lollobrigida *et al.* reported the presence of titanium particles on the titanium surfaces after using a titanium brush for instrumentation [52]. Emerging evidence suggests that titanium particles released from the implant surface may contribute to undesirable biological events, such as the development of peri-implantitis and osteolysis[53,54].

4.2. Surface elemental composition

Titanium implants are typically constructed from commercially pure titanium (cpTi) or titanium alloys. Among these, cpTi is predominantly used because of its excellent biocompatibility and lower cost. However, grade V titanium alloys, such as Ti 6Al-4V, are frequently favoured for their superior mechanical properties [55]. In our experiment, we selected the Ti 6Al-4V alloy because various commercial implants with SLA surfaces are constructed from the same alloy, and this experiment aims to investigate the effect of different rotary brushes on SLA titanium surfaces.

The implant surface elemental composition is mainly influenced by the bulk material used for the fabrication of the implant. Despite this, the surface composition may vary due to surface reactivity and selective elements display [56]. The corrosion resistance of titanium implants stems from titanium's affinity toward oxygen, which results in the formation of a thin layer of titanium oxide that protects the underlying bulk material from the environment [57]. The implant surface chemical composition is also modified to influence cellular responses to favour rapid and uneventful osseointegration [58]. Therefore, alterations in the implant surface elemental composition following mechanical decontamination may impact the implant corrosion resistance and the

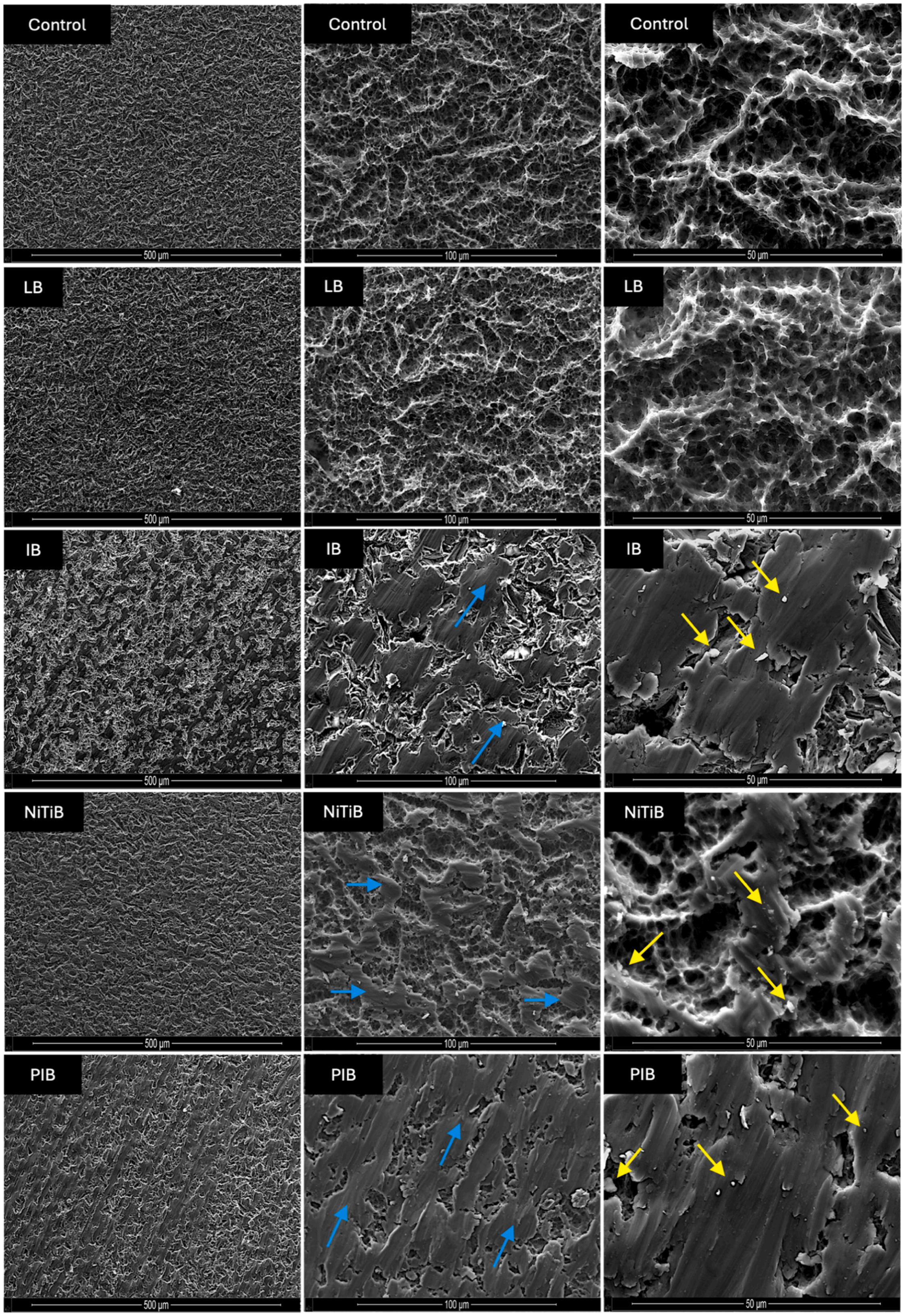

Fig. 4. SEI of titanium surfaces after mechanical instrumentation. The blue arrows indicate the flattened portions and direction in which the mechanical instrumentation was performed. The yellow arrows demonstrate loose, abraded titanium particles. Magnification scale bar 500µm, 100 µm, 50 µm (from left to right).

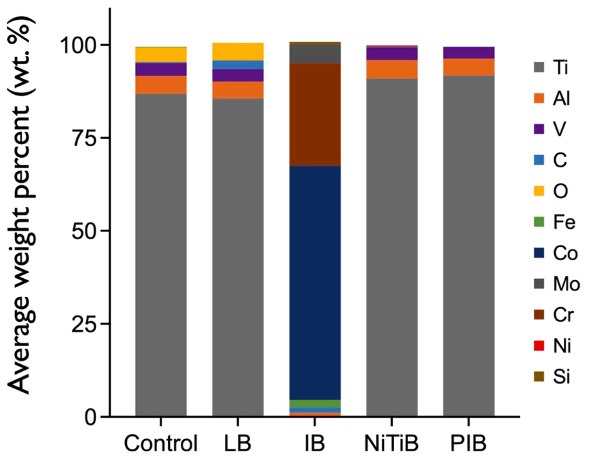

Fig. 5. Graphical representation of average atomic weights (wt%) of elemental composition after mechanical instrumentation.

re-osseointegration process. In this experiment, we find various contaminants on the instrumented titanium surfaces. In the LB group, higher carbon and oxygen content are observed on the instrumented surfaces due to the detachment and breakage of brush bristles during instrumentation. The surfaces of the IB group exhibit a unique elemental composition due to the stainless steel bristles of the brush, which deposit its contents on the surfaces during instrumentation. Stainless steel components such as cobalt (Co), chromium (Cr), molybdenum (Mo), and iron (Fe) are detected on the surfaces of the IB group. Likewise, nickel (Ni) is present on titanium surfaces treated with NiTiB, reflecting the nickel-titanium alloy composition of the brush bristles. During the instrumentation process in the NiTiB and PIB groups, loose titanium particles are produced, possibly leading to the slightly elevated titanium levels in these groups. The decontamination process and the bristle composition seem to influence the surface elemental composition of the decontaminated titanium surfaces.

4.3. Surface roughness

The use of rotary brushes has been indicated, by some authors, as a protocol with high decontamination potential that does not lead to significant surface roughness changes [59–61]. In our experiment, we observed that rotary brushes altered the surface roughness, resulting in a smoothening effect that makes the SLA titanium surface less rough. In line with our observation, many authors reported smoother titanium surfaces after using titanium brushes for mechanical decontamination [50,51,62–64]. This alteration in surface roughness can modify cellular responses, which could negatively impact the re-osseointegration process [65,66]. The trend in surface smoothening is closely related to the rotation speed used during instrumentation. The IB produced the smoothest surface among the decontamination groups, which can be explained by the high rotation speed of 5500 rpm. On the other hand, the PIB and NiTiB reduced surface roughness to a lesser extent due to the lower rotation speeds of 2000 and 800 rpm, respectively. In contrast to our findings, Park *et al.* found that instrumenting titanium surfaces with titanium brush did not change the surface roughness [61]. This difference in the effect can be attributed to the instrumentation protocol used, where a rotation speed of 300 rpm was used for 30 s in the study mentioned above, while a higher speed was used in our experiment for 60 s.

4.4. Surface wettability

Material surface wettability has recently received more attention in dental implant applications as a feature impacting osseointegration. Implants with high-energy surfaces are believed to promote interactions with the biological environment, facilitating rapid osseointegration [56]. In our study, we find that all metallic brushes enhance surface wettability and render the titanium surfaces more hydrophilic, confirming the findings of previous reports [49–51]. Interdependencies exist among implant surface properties; thus, modifying one property results in the alteration of others [67]. Based on this, it is plausible to find that IB had the greatest impact on surface wettability because it has significantly changed surface topography and elemental composition. Using metallic rotary brushes for implant surface decontamination represents a potential biological benefit as it improves implant surface wettability. However, most of the clinically marketed dental implants

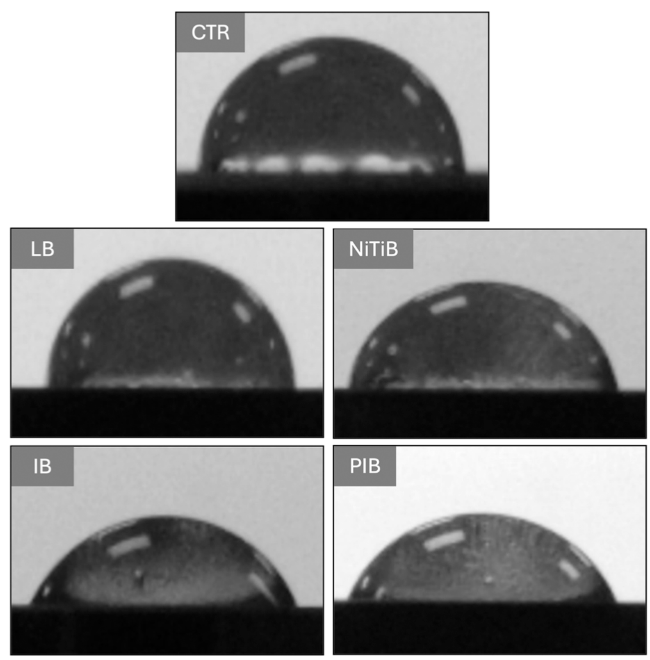

Fig. 6. Representative images of surface wettability employing water droplets.

Table 2
Topographical characterisation by roughness parameters and wettability (θ°).

Group	Sa $_{(\mu m)}$ Median (Range)	Sz $_{(\mu m)}$ Median (Range)	Ssk $_{(\mu m)}$ Median (Range)	Sku Median (Range)	Sdq $_{(\mu m)}$ Median (Range)	Sdr $_{(\%)}$ Median (Range)	Contact angle (θ°) Median (Range)
CTR	1.53 (0.12)^{A}	20.96 (15.39)^{A}	−0.25 (0.60)^{A}	3.40 (0.86)^{A}	2.39 (0.48)^{A}	121.10 (20)^{A}	84.8 (21.0)^{A}
LB	1.49 (0.21)^{A}	20.74 (9.03)^{A}	−0.26 (0.22)^{A}	3.35 (0.53)^{A}	2.69 (.02)^{B}	134.99 (38.56)^{B}	85.9 (17.0)^{A}
IB	0.88 (0.57)^{B}	17 (13.43)^{B}	−1.14 (2.02)^{B}	6.88 (5.32)^{B}	1.81 (.93)^{C}	63.27 (61.32)^{C}	67.45 (12.50)^{B}
NiTiB	1.41 (0.28)^{C}	17.16 (12.60)^{BC}	−0.75 (0.53)^{C}	3.46 (1.29)^{A}	2.32 (0.49)^{A}	103.47 (26.93)^{D}	81.0 (18.3)^{C}
PIB	1.28 (0.23)^{D}	18.81 (11.98)^{BD}	−0.54. (.99)^{D}	3.98 (5.87)^{C}	2.17 (0.34)^{D}	90.08 (20.35)^{E}	65.3 (25.7)^{BD}
P-value[a]	< 0.001*	< 0.001*	< 0.001*	< 0.001*	< 0.001*	< 0.001*	< 0.001*

[a] Kruskal-Wallis with Dunn-Bonferroni post hoc tests, *$p < 0.05$.
For each column, cells with different superscript letters indicate significant statistical differences between the decontamination groups ($p < 0.05$).

are hydrophobic, and the impact of enhancing the implant wettability on re-osseointegration is still unclear [56,58,68].

This study has certain limitations. Firstly, titanium discs were used instead of dental implants to ensure more precise surface characterisation, as working on implants with screw threads can be challenging. Additionally, only SLA titanium surfaces were examined, potentially limiting the applicability of our findings to other implant surfaces.

5. Conclusion

Mechanical decontamination of implant surfaces utilising rotary brushes can alter implant surface properties. The brush material, design, and decontamination parameters, such as rotational speed, influence their effect on implant surface properties. i-Brush1, NiTiBrush Nano, and peri-implantitis brushes induced significant alterations in titanium implant surface properties, while Labrida BioClean brush demonstrated minimal impact on surface properties.

Declaration of Competing Interest

This research received funding from the Saudi Arabian Cultural Bureau in London, UK, in support of the first author, Mohammed Alabbad. The funder had no role in the study design, data collection and analysis, decision to publish, or manuscript preparation.

References

[1] Howe MS, Keys W, Richards D. Long-term (10-year) dental implant survival: A systematic review and sensitivity meta-analysis. J Dent 2019;84:9–21.
[2] Wang Y, Bäumer D, Ozga AK, Körner G, Bäumer A. Patient satisfaction and oral health-related quality of life 10 years after implant placement. BMC Oral Health 2021;21:30.
[3] Berglundh T, Persson L, Klinge B. A systematic review of the incidence of biological and technical complications in implant dentistry reported in prospective longitudinal studies of at least 5 years. J Clin Periodo 2002;29:197–212.
[4] Derks J, Tomasi C. Peri-implant health and disease. A systematic review of current epidemiology. J Clin Periodo 2015;42. S158-S71.
[5] Lee CT, Huang YW, Zhu L, Weltman R. Prevalences of peri-implantitis and peri-implant mucositis: systematic review and meta-analysis. J Dent 2017;62:1–12.
[6] Jung RE, Zembic A, Pjetursson BE, Zwahlen M, Thoma DS. Systematic review of the survival rate and the incidence of biological, technical, and aesthetic complications of single crowns on implants reported in longitudinal studies with a mean follow-up of 5 years. Clin Oral Implants Res 2012;23(6):2–21.
[7] Diaz P, Gonzalo E, Villagra LJG, Miegimolle B, Suarez MJ. What is the prevalence of peri-implantitis? A systematic review and meta-analysis. BMC Oral Health 2022;22:449.
[8] Heitz-Mayfield L, Lang NP. Comparative biology of chronic and aggressive periodontitis vs. peri-implantitis. Periodontal 2000 2010;53:167–81.
[9] Carvalho ÉBS, Romandini M, Sadilina S, Sant'Ana ACP, Sanz M. Microbiota associated with peri-implantitis-A systematic review with meta-analyses. Clin Oral Implants Res 2023;34:1176–87.
[10] Berglundh T, Armitage G, Araujo MG, Avila-Ortiz G, Blanco J, Camargo PM, et al. Peri-implant diseases and conditions: Consensus report of workgroup 4 of the 2017 World Workshop on the Classification of Periodontal and Peri-Implant Diseases and Conditions. J Clin Periodo 2018;45(20):S286–s91.
[11] Figuero E, Graziani F, Sanz I, Herrera D, Sanz M. Management of peri-implant mucositis and peri-implantitis. Periodontal 2000 2014;66:255–73.
[12] Renvert S, Polyzois IN. Clinical approaches to treat peri-implant mucositis and peri-implantitis. Periodontol 2000 2015;68:369–404.
[13] Monje A, Amerio E, Cha JK, Kotsakis G, Pons R, Renvert S, et al. Strategies for implant surface decontamination in peri-implantitis therapy. Int J Oral Implant (Berl) 2022;15:213–48.
[14] Ramanauskaite A, Schwarz F, Cafferata EA, Sahrmann P. Photo/mechanical and physical implant surface decontamination approaches in conjunction with surgical peri-implantitis treatment: A systematic review. J Clin Periodo 2023;50:317–35.
[15] Herrera D, Berglundh T, Schwarz F, Chapple I, Jepsen S, Sculean A, et al. Prevention and treatment of peri-implant diseases—The EFP S3 level clinical practice guideline. J Clin Periodo 2023;50:4–76.
[16] Louropoulou A, Slot DE, Weijden F. The effects of mechanical instruments on contaminated titanium dental implant surfaces: a systematic review. Clin Oral Implants Res 2014;25:1149–60.
[17] Louropoulou A, Slot DE, Van der Weijden F. Influence of mechanical instruments on the biocompatibility of titanium dental implants surfaces: a systematic review. Clin Oral Implants Res 2015;26:841–50.
[18] Wennerberg A, Albrektsson T, Andersson B, Krol J. A histomorphigenetric study of screw-shaped and removal torque titanium implants with three different surface topographies. Clin Oral Implants Res 1995;6:24–30.
[19] Quirynen M, Marechal M, Busscher H, Weerkamp A, Darius P, van Steenberghe D. The influence of surface free energy and surface roughness on early plaque formation: an in vivo study in man. J Clin Periodo 1990;17:138–44.
[20] Brett P, Harle J, Salih V, Mihoc R, Olsen I, Jones F, et al. Roughness response genes in osteoblasts. Bone 2004;35:124–33.
[21] Buser D, Broggini N, Wieland M, Schenk R, Denzer A, Cochran D, et al. Enhanced bone apposition to a chemically modified SLA titanium surface. J Dent Res 2004;83:529–33.
[22] Bagno A, Di Bello C. Surface treatments and roughness properties of Ti-based biomaterials. J Mater Sci:Mater Med 2004;15:935–49.
[23] Jayaraman M, Meyer U, Bühner M, Joos U, Wiesmann H-P. Influence of titanium surfaces on attachment of osteoblast-like cells in vitro. Biomaterials 2004;25:625–31.
[24] Sammons RL, Lumbikanonda N, Gross M, Cantzler P. Comparison of osteoblast spreading on microstructured dental implant surfaces and cell behaviour in an explant model of osseointegration: a scanning electron microscopic study. Clin Oral Implants Res 2005;16:657–66.
[25] Teughels W, Van Assche N, Sliepen I, Quirynen M. Effect of material characteristics and/or surface topography on biofilm development. Clin Oral Implants Res 2006;17:68–81.
[26] Köunönen M, Hormia M, Kivilahti J, Hautaniemi J, Thesleff I. Effect of surface processing on the attachment, orientation, and proliferation of human gingival fibroblasts on titanium. J Biomed Mater Res 1992;26:1325–41.
[27] Mustafa K, Lopez BS, Hultenby K, Wennerberg A, Arvidson K. Attachment and proliferation of human oral fibroblasts to titanium surfaces blasted with TiO2 particles. A scanning electron microscopic and histomorphometric analysis. Clin Oral Implants Res 1998;9:195–207.
[28] Le Guéhennec L, Soueidan A, Layrolle P, Amouriq Y. Surface treatments of titanium dental implants for rapid osseointegration. Dent Mater 2007;23:844–54.
[29] Junker R, Dimakis A, Thoneick M, Jansen JA. Effects of implant surface coatings and composition on bone integration: a systematic review. Clin Oral Implants Res 2009;20(4):185–206.
[30] Moharrami M, Perrotti V, Iaculli F, Love RM, Quaranta A. Effects of air abrasive decontamination on titanium surfaces: A systematic review of in vitro studies. Clin Implant Dent Relat Res 2019;21:398–421.
[31] Louropoulou A, Slot DE, Van Der Weijden FA. Titanium surface alterations following the use of different mechanical instruments: a systematic review. Clin Oral Implants Res 2012;23:643–58.
[32] John G, Becker J, Schwarz F. Effectivity of air-abrasive powder based on glycine and tricalcium phosphate in removal of initial biofilm on titanium and zirconium oxide surfaces in an ex vivo model. Clin Oral Invest 2016;20:711–9.
[33] Koishi R, Taguchi Y, Okuda M, Tanaka A, Umeda M. Behavior of human gingival epithelial cells on titanium following abrasion of the adjunctive glycine air polishing powder. J Hard Tissue Biol 2016;25:205–12.
[34] Drago L, Del Fabbro M, Bortolin M, Vassena C, De Vecchi E, Taschieri S. Biofilm removal and antimicrobial activity of two different air-polishing powders: An in vitro study. J Periodontal 2014;85:e363–9.
[35] Shibli JA, Silverio KG, Martins MC, Marcantonio JrE, Rossa JrC. Effect of air-powder system on titanium surface on fibroblast adhesion and morphology. Implant Dent 2003;12:81–6.
[36] Meyle J. Mechanical, chemical and laser treatments of the implant surface in the presence of marginal bone loss around implants. Eur J Oral Implant 2012;5.
[37] Koo K-T, Khoury F, Keeve PL, Schwarz F, Ramanauskaite A, Sculean A, et al. Implant surface decontamination by surgical treatment of periimplantitis: A literature review. Implant Dent 2019;28:173–6.
[38] Wohlfahrt JC, Lyngstadaas SP. Mechanical debridement of a peri-implant osseous defect with a novel titanium brush and reconstruction with porous titanium granules: a case report with reentry surgery. Clin Adv Periodontics 2012;2:136–40.
[39] de Tapia B, Valles C, Ribeiro-Amaral T, Mor C, Herrera D, Sanz M, et al. The adjunctive effect of a titanium brush in implant surface decontamination at peri-implantitis surgical regenerative interventions: A randomized controlled clinical trial. J Clin Periodo 2019;46:586–96.
[40] Neely AL, Thompson TN, Gupta V, Kinaia B. Successful management of peri-implantitis using a titanium brush and a doxycycline-saline slurry for surface detoxification with guided bone regeneration: a 5-year follow-up. Clin Adv Periodontics 2020;10:118–22.
[41] Koldsland OC, Aass AM. Supportive treatment following peri-implantitis surgery: An RCT using titanium curettes or chitosan brushes. J Clin Periodo 2020;47:1259–67.
[42] Duddeck D, Karapetian V, Grandoch A. Time-saving debridment of implants with rotating titanium brushes. Implants 2012;3:20–2.
[43] Ramanauskaite A, Schwarz F, Cafferata EA, Sahrmann P. Photo/mechanical and physical implant surface decontamination approaches in conjunction with surgical peri-implantitis treatment: A systematic review. J Clin Periodo 2023;50(26):317–35.
[44] Baima G, Citterio F, Romandini M, Romano F, Mariani GM, Buduneli N, et al. Surface decontamination protocols for surgical treatment of peri-implantitis: A systematic review with meta-analysis. Clin Oral Implants Res 2022;33:1069–86.
[45] González FJ, Requena E, Miralles L, Sanz JL, Barberá J, Enciso JJ, et al. Adjuvant effect of titanium brushes in peri-implant surgical treatment: a systematic review. Dent J (Basel) 2021;9.
[46] Wohlfahrt JC, Aass AM, Koldsland OC. Treatment of peri-implant mucositis with a chitosan brush-A pilot randomized clinical trial. Int J Dent Hyg 2019;17:170–6.
[47] Khan SN, Koldsland OC, Roos-Jansåker AM, Wohlfahrt JC, Verket A, Mdala I, et al. Non-surgical treatment of mild to moderate peri-implantitis using an oscillating

chitosan brush or a titanium curette-A randomized multicentre controlled clinical trial. Clin Oral Implants Res 2022;33:1254–64.
[48] Wennerberg A, Albrektsson T. Suggested guidelines for the topographic evaluation of implant surfaces. Int J Oral Maxillofac Implants 2000;15.
[49] Eun S-M, Son K, Hwang S-M, Son Y-T, Kim Y-G, Suh J-Y, et al. The impact of mechanical debridement techniques on titanium implant surfaces: a comparison of sandblasted, acid-etched, and femtosecond laser-treated surfaces. J Funct Biomater 2023;14:502.
[50] Sousa V, Mardas N, Spratt D, Hassan IA, Walters NJ, Beltrán V, et al. The effect of microcosm biofilm decontamination on surface topography, chemistry, and biocompatibility dynamics of implant titanium surfaces. Int J Mol Sci 2022;23.
[51] Bayrak M, Kocak-Oztug NA, Gulati K, Cintan S, Cifcibasi E. Influence of clinical decontamination techniques on the surface characteristics of SLA titanium implant. Nanomater (Basel) 2022;12.
[52] Lollobrigida M, Fortunato L, Serafini G, Mazzucchi G, Bozzuto G, Molinari A, et al. The prevention of implant surface alterations in the treatment of peri-implantitis: comparison of three different mechanical and physical treatments. Int J Environ Res Public Health 2020;17.
[53] Eger M, Sterer N, Liron T, Kohavi D, Gabet Y. Scaling of titanium implants entrains inflammation-induced osteolysis. Sci Rep 2017;7:39612.
[54] Chen L, Tong Z, Luo H, Qu Y, Gu X, Si M. Titanium particles in peri-implantitis: distribution, pathogenesis and prospects. Int J Oral Sci 2023;15:49.
[55] Osman RB, Swain MV. A critical review of dental implant materials with an emphasis on titanium versus zirconia. Mater (Basel) 2015;8:932–58.
[56] Gittens RA, Scheideler L, Rupp F, Hyzy SL, Geis-Gerstorfer J, Schwartz Z, et al. A review on the wettability of dental implant surfaces II: Biological and clinical aspects. Acta Biomater 2014;10:2907–18.
[57] Sul YT, Johansson C, Wennerberg A, Cho LR, Chang BS, Albrektsson T. Optimum surface properties of oxidized implants for reinforcement of osseointegration: surface chemistry, oxide thickness, porosity, roughness, and crystal structure. Int J Oral Maxillofac Implants 2005;20:349–59.
[58] Albrektsson T, Wennerberg A. On osseointegration in relation to implant surfaces. Clin Implant Dent Relat Res 2019;21(1):4–7.
[59] Toma S, Behets C, Brecx MC, Lasserre JF. In vitro comparison of the efficacy of peri-implantitis treatments on the removal and recolonization of streptococcus gordonii biofilm on titanium disks. Mater (Basel) 2018;11.
[60] John G, Becker J, Schwarz F. Rotating titanium brush for plaque removal from rough titanium surfaces–an in vitro study. Clin Oral Implants Res 2014;25:838–42.
[61] Park JB, Jeon Y, Ko Y. Effects of titanium brush on machined and sand-blasted/acid-etched titanium disc using confocal microscopy and contact profilometry. Clin Oral Implants Res 2015;26:130–6.
[62] Stuani VT, Kim DM, Nagai M, Chen CY. Sant'Ana ACP. Effectiveness and surface changes of different decontamination protocols at smooth and minimally rough titanium surfaces. J Periodo 2021;92:704–15.
[63] Tavakoli M, Yaghini J, Izadi M, Molavi H, Sabet NK. Effects of titanium curette, air polishing and titanium brush on implant surface roughness using scanning probe microscopy. Avicenna J Dent Res 2019;11:21–5.
[64] Kim YS, Park JB, Ko Y. Surface alterations following instrumentation with a nylon or metal brush evaluated with confocal microscopy. J Periodontal Implant Sci 2019;49:310–8.
[65] Wennerberg A, Albrektsson T. Effects of titanium surface topography on bone integration: a systematic review. Clin Oral Implants Res 2009;20:172–84.
[66] Wennerberg A, Albrektsson T. On implant surfaces: a review of current knowledge and opinions. Int J Oral Maxillofac Implants 2010;25:63–74.
[67] Ponche A, Bigerelle M, Anselme K. Relative influence of surface topography and surface chemistry on cell response to bone implant materials. Part 1: physico-chemical effects. Proc Inst Mech Eng H 2010;224:1471–86.
[68] Rupp F, Scheideler L, Eichler M, Geis-Gerstorfer J. Wetting behavior of dental implants. Int J Oral Maxillofac Implants 2011;26:1256–66.